Weakened tropical circulation and reduced precipitation in response to geoengineering

Weakened tropical circulation and reduced precipitation in response to geoengineering

Angus J Ferraro, Eleanor J Highwood and Andrew J Charlton-Perez

Department of Meteorology, University of Reading, Reading, UK

E-mail: a.j.ferraro@pgr.reading.ac.uk

Abstract

Geoengineering by injection of reflective aerosols into the stratosphere has been proposed as a way to counteract the warming effect of greenhouse gases by reducing the intensity of solar radiation reaching the surface. Here, climate model simulations are used to examine the effect of geoengineering on the tropical overturning circulation. The strength of the circulation is related to the atmospheric static stability and has implications for tropical rainfall. The tropical circulation is projected to weaken under anthropogenic global warming. Geoengineering with stratospheric sulfate aerosol does not mitigate this weakening of the circulation. This response is due to a fast adjustment of the troposphere to radiative heating from the aerosol layer. This effect is not captured when geoengineering is modelled as a reduction in total solar irradiance, suggesting caution is required when interpreting model results from solar dimming experiments as analogues for stratospheric aerosol geoengineering.

S Online supplementary data available from stacks.iop.org/ERL/9/014001/mmedia

1. Introduction

Earth's climate is projected to warm during the 21st century as a consequence of human emissions of greenhouse gases [1]. However, little progress has been made in reducing the emissions of these gases, leading to discussion of geoengineering by reducing incoming solar radiation as a potential policy option [2, 3]. Modelling studies have shown that geoengineering using stratospheric aerosols has the potential to reduce Earth's global-mean surface temperature [4, 5], but that using geoengineering to counterbalance surface warming from carbon dioxide (CO_2) decreases global-mean precipitation [6, 7]. The effects of stratospheric aerosol geoengineering are also regionally inhomogeneous [8, 9], which raises questions of how geoengineering might be deployed equitably. Climate changes on these regional scales are influenced by changes in atmospheric circulation as well as global atmospheric radiative effects.

The regional response of tropical precipitation to climate change is determined by changes in atmospheric humidity and vertical motion. Greenhouse warming increases specific humidity, which acts to increase precipitation in convective systems. Conversely, the tropical circulation is expected to weaken under greenhouse warming [10, 11] because CO_2 warms the mid-troposphere more than the surface, stabilizing the atmosphere [12]. This allows for stronger adiabatic cooling by upwelling motions, reducing the amount of convective upwelling needed to balance atmospheric

heating [13]. Such a weakening of the tropical circulation, in the absence of surface warming and humidity changes, would act to reduce precipitation in convective regions [14]. Bony *et al* [14] quantify this 'dynamic' component of precipitation change and suggest that sunlight reflection geoengineering schemes, since they do not remove CO_2 from the atmosphere, should not be expected to counteract CO_2-driven precipitation change on a regional scale. Precipitation changes due to surface temperature change, however, would disappear. The first question we address in this study is: to what extent do solar geoengineering schemes mitigate tropical precipitation changes due to CO_2 increases?

Multi-model assessments of the precipitation response to geoengineering to date have mostly modelled geoengineering as a reduction in solar irradiance, as in the 'G1' specification of the Geoengineering Model Intercomparison Project [15]. They show that, when a reduction in solar irradiance is used to counterbalance the surface warming produced by a quadrupling of CO_2 concentrations, global-mean precipitation is reduced, with regionally inhomogeneous changes which are relatively small compared to those produced by continued greenhouse warming [16–18]. However, since the feasibility of reduction in solar irradiance external to the atmosphere is limited, it is important to assess the applicability of such model experiments to geoengineering with stratospheric aerosols. This leads us to the second question addressed in this study: does reducing solar irradiance correctly represent the effects of stratospheric aerosol geoengineering on the tropical temperature profile and consequently on the tropical circulation and precipitation?

2. Methods

We address this question by comparing simulations of high-CO_2 and geoengineered climates using the University of Reading Intermediate General Circulation Model (IGCM) [19], an intermediate-complexity climate model with simplified physical parameterizations that retain enough complexity to realistically simulate Earth's precipitation climatology (see supplementary material, figure S1 available at stacks.iop.org/ERL/9/014001/mmedia).

2.1. Climate model simulations

The IGCM is a spectral model which uses triangular truncation of spherical harmonics at wavenumber 42 (T42) and has 35 vertical levels up to 0.1 hPa. It uses the Morcrette [20] radiation scheme to calculate diurnally averaged radiative fluxes. The six spectral regions in the LW are: 0–350 cm^{-1} and 1450–1880 cm^{-1}, 500–800 cm^{-1}, 800–970 cm^{-1} and 1110–1250 cm^{-1}, 970–1110 cm^{-1}, 350–500 cm^{-1}, 1250–1450 cm^{-1} and 1880–2820 cm^{-1}. The spectral regions in the SW are: 0.25–0.68 μm (visible), 0.68–4.00 μm (near-infrared). Absorption coefficients for ozone, water vapour and well-mixed greenhouse gases are derived from the HITRAN [21] database.

The IGCM is here used in three sets of simulations.

(1) *Slab ocean*. The IGCM is coupled to a static mixed-layer 'slab' ocean 100 m deep to simulate the equilibrium response of the climate system to geoengineering. Ocean heat fluxes are calculated from the surface energy imbalance when the IGCM is run with a monthly sea surface temperature climatology from the ERA-40 reanalysis [22]. Each simulation is 80 years long. The global-mean surface temperature equilibrates after 15 years, so the final 65 years of each simulation are used for equilibrium analysis.

(2) *Fixed-surface-temperature*. In order to calculate the fast radiative effect of changing atmospheric constituents, short (three-year) simulations are conducted with the same forcings as the slab ocean simulations, but with ocean and land surface temperatures fixed using data from the ECMWF ERA-40 reanalysis [22]. Only three years are required because the atmosphere responds much more quickly than the ocean to radiative forcings. The final two years of these simulations are analysed.

(3) *Instantaneous radiative heating rate calculations*. The instantaneous radiative heating rate perturbations in the IGCM are calculated using single-timestep simulations with fixed surface temperatures. A single-timestep run is initialized every three days from the control run, giving a total of 120 single-timestep calculations of the instantaneous heating rates over one calendar year. The mean heating rate perturbation is then calculated by averaging over these 120 simulations and subtracting the climatology from the control.

We simulate four climates, including a 20th century control and a simulation with quadrupled CO_2 concentrations ('4CO_2'). We compare '4CO_2' with two simulations of geoengineering in which the surface warming from a quadrupling of CO_2 is counterbalanced. '4CO_2 + Solar' uses solar irradiance reduction similarly to the GeoMIP G1 specification to counterbalance the warming from a quadrupling of CO_2 (the GeoMIP specification requires the global-mean surface temperature to be returned to pre-industrial levels, rather than the 20th century baseline used here). '4CO_2 + Sulfate' uses a prescribed layer of sulfate aerosol placed in the lower stratosphere (figure 1) to return the global-mean surface temperature to 20th century baseline. Hence the global-mean surface temperature changes are near-zero in both these simulations (0.10 K for '4CO_2 + Solar' and −0.28 K for '4CO_2 + Sulfate' compared to 4.20 K for '4CO_2'; table 1).

2.2. Sulfate aerosol distribution

In the 'sulfate' integrations a zonally uniform aerosol distribution is prescribed in the lower stratosphere. The aerosol mass mixing ratio peaks in the tropics at the assumed location of injection of sulfate aerosol (or some precursor such as sulfur dioxide), approximately 50 hPa. Figure 1 shows the aerosol mass mixing ratio as a function of latitude and
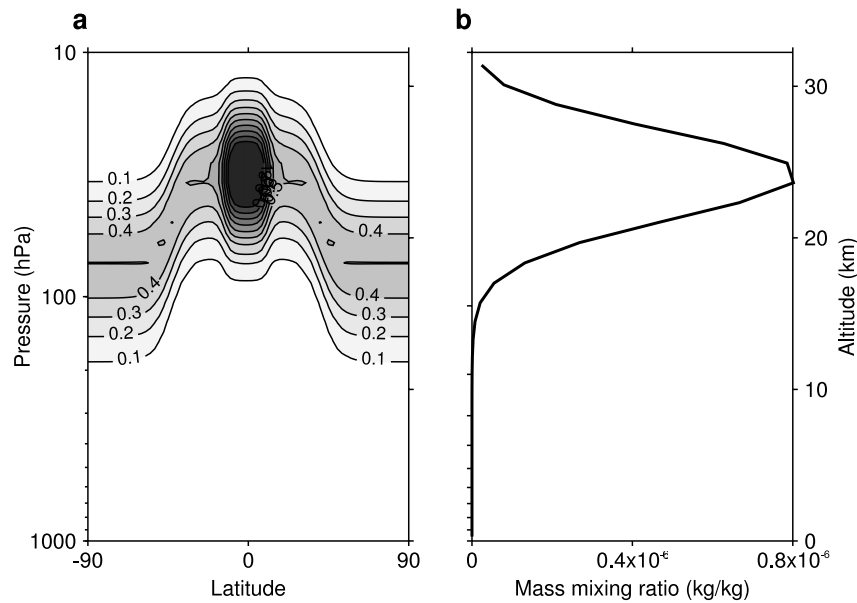
a

b

Figure 1. (a) Zonal-mean sulfate aerosol mass mixing ratio in units of 10^{-6} kg kg^{-1}, (b) area-weighted tropical-mean (30S–30N).

Table 1. Surface temperature and precipitation responses.

Simulation	CO_2 (ppmv)	Geoengineering	Global-mean surface temperature change (K)	Tropical-mean (30S–30N) surface temperature change (K)	Tropical-mean (30S–30N) precipitation change (mm d^{-1})
Control	350	—	0	0	0
4CO_2	1400	—	4.20	3.33	0.16
4CO_2 + Sulfate	1400	Prescribed sulfate aerosol layer in lower stratosphere (see section 2)	−0.28	0.04	−0.25
4CO_2 + Solar	1400	Reduction in total solar irradiance of 3.4%	0.10	−0.21	−0.14

altitude. It qualitatively represents the main features of a geoengineering sulfate aerosol layer simulated by aerosol transport models [23]. The aerosol layer is formed using an analytical function of latitude and altitude, details of which are given in the supplementary material (available at stacks. iop.org/ERL/9/014001/mmedia).

The radiative characteristics of the aerosol are calculated according to Mie theory assuming a lognormal size distribution with median radius 0.1 μm and a geometric standard deviation of 2.0. There is considerable uncertainty, however, over the size to which sulfate aerosol will grow in the stratosphere. The aerosol median radius increases with injection rate as a result of coagulation processes which decreases its lifetime in the stratosphere [23]. Increasing the rate of injection of aerosol in the stratosphere therefore gives diminishing returns in terms of radiative forcing. Scattering efficiency is also reduced for large aerosols, suggesting there is a maximum attainable radiative forcing for stratospheric injection of sulfate aerosol. It is therefore unclear whether a cooling sufficient to counterbalance the surface warming from a quadrupling of CO_2 could be achieved with sulfate aerosol. Our simulations, therefore, are highly idealized, representing

a geoengineering scenario that may not be technologically achievable. We use these idealized simulations to obtain a clear signal of the response of the climate system to geoengineering forcings and to identify the physical processes determining this response, but also discuss sensitivity of the results to the aerosol size distributions throughout the results.

3. Results

We first consider the effect of climate perturbations on the tropical temperature profile. Quadrupling CO_2 warms the entire tropical (30S–30N) troposphere (figure 2(a)). The equilibrium warming reaches a peak of approximately 6.5 K at 250 hPa, about twice the 3.33 K surface warming. The resultant increase in static stability comes from two sources: a 'fast radiative' effect from net atmospheric heating by CO_2 [24, 25] and a 'surface-mediated' increased latent heating of the atmosphere caused by increased tropospheric specific humidity. The surface-mediated effect grows as the surface warms, as shown by the thin lines in figure 2. The contribution of the fast radiative effect to the tropospheric temperature change is calculated using three-year simulations
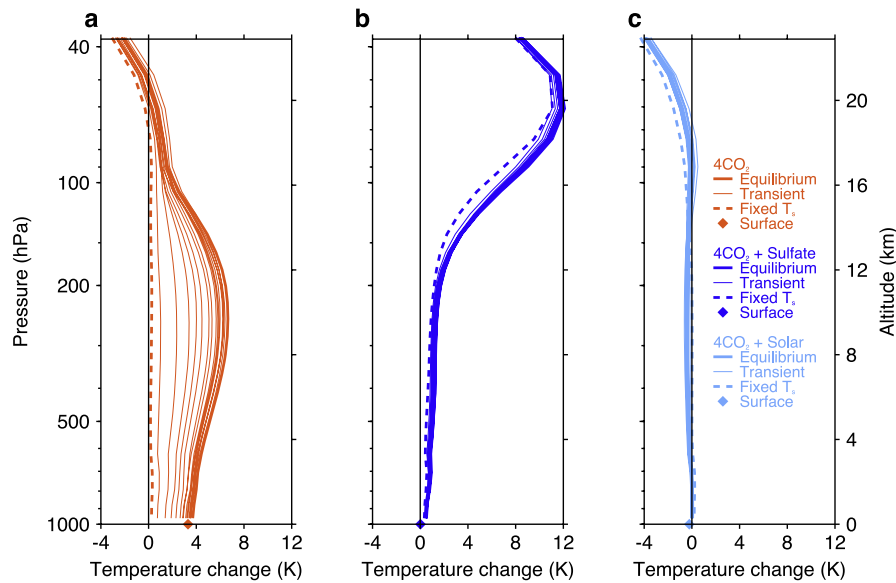
Figure 2. Vertical profiles of tropical-mean temperatures changes compared to the control simulation for (a) $4CO_2$, (b) $4CO_2$ + Sulfate and (c) $4CO_2$ + Solar. Thin lines show the evolution of the temperature profile change over time, with one line representing the annual mean for each of the first 15 years of the simulation. Dashed lines show simulations with fixed-surface-temperature (T_s).

in which the surface temperature is fixed (dashed lines in figure 2). This simulation reveals that the fast radiative effect of CO_2 contributes approximately 0.1 K of the tropospheric warming, with the majority caused by the 'surface-mediated' effect of latent heat release.

The two geoengineering simulations show very different profiles of tropical-mean temperature change. Sulfate geoengineering (figure 2(b), thick solid line) warms the troposphere, whereas solar dimming (figure 2(c)) produces slight tropospheric cooling. Note that both geoengineering simulations also have quadrupled atmospheric CO_2 concentrations and therefore include the fast radiative effect of CO_2 on the atmosphere.

The temperature change in '$4CO_2$' peaks around 250 hPa and then decreases with height. In contrast, the '$4CO_2$ + Sulfate' warming increases with height. The warming is established within the first year of the simulation, with the fast radiative effect of the combination of sulfate and CO_2 being greater than that of CO_2 alone. The additional process in the geoengineering is the absorption and emission of LW radiation [26], which produces stratospheric heating in '$4CO_2$ + Sulfate'. '$4CO_2$ + Sulfate' therefore increases the downwelling longwave radiation both by enhanced emission from the aerosol itself, and by enhanced emission from other constituents in the warmer stratosphere.

Instantaneous heating rate calculations (see section 2.1) can be used to show the fast radiative effect of the perturbations before atmospheric or surface temperatures have adjusted. The heating rates for the three simulations all show CO_2-induced warming of the troposphere (figure 3), consistent with the fast radiative effect calculated in the $4CO_2$ fixed-surface-temperature simulation (dashed line in figure 2(a)). The '$4CO_2$ + Solar' simulation produces a very similar heating rate perturbation to $4CO_2$, though slightly reduced due to decreased downwelling solar radiation

(figure 3(c)), which reduces near-infrared absorption by water vapour [27].

The '$4CO_2$ + Sulfate' simulation produces greater longwave (LW; 4–50 μm) tropospheric heating than '$4CO_2$' (figure 3(b)). The heating decreases approximately linearly with height from 0.1 K d^{-1} at 100 hPa to 0.05 K d^{-1} at 600 hPa. Consistent with aerosol transport modelling of a geoengineering aerosol layer [28], some of the aerosol in our prescribed distribution reaches below 100 hPa (supplementary figure 1 available at stacks.iop.org/ERL/9/014001/mmedia). The upper-tropospheric heating, however, is not a result of radiative absorption by the aerosol because the aerosol concentration decreases exponentially into the troposphere, rather than linearly like the heating rate perturbation. The upper-tropospheric heating is instead a consequence of increased downward LW emission by the aerosol itself. The emitted LW radiation is absorbed in the troposphere by radiatively active gases (principally water vapour) enhancing radiative heating. This radiative heating (figure 3) does not increase as strongly with height as the temperature change (figure 2(b)). This may be partly due to changing radiative relaxation rates with altitude, but also because the effect on the downwelling LW of stratospheric warming caused by the aerosols (as seen in figure 2, this warming peaks at approximately 40 hPa) is not included in these instantaneous calculations.

Under increasing CO_2 concentrations the static stability of the troposphere is increased, as shown by the enhanced upper-tropospheric warming in figure 2(a). Under stratospheric aerosol geoengineering this stabilization remains, but instead of coming from moist adiabatic adjustment to surface warming it comes from increased LW tropospheric radiative heating. This heating comes from increased downwelling LW radiation and has two sources: emission from the aerosol
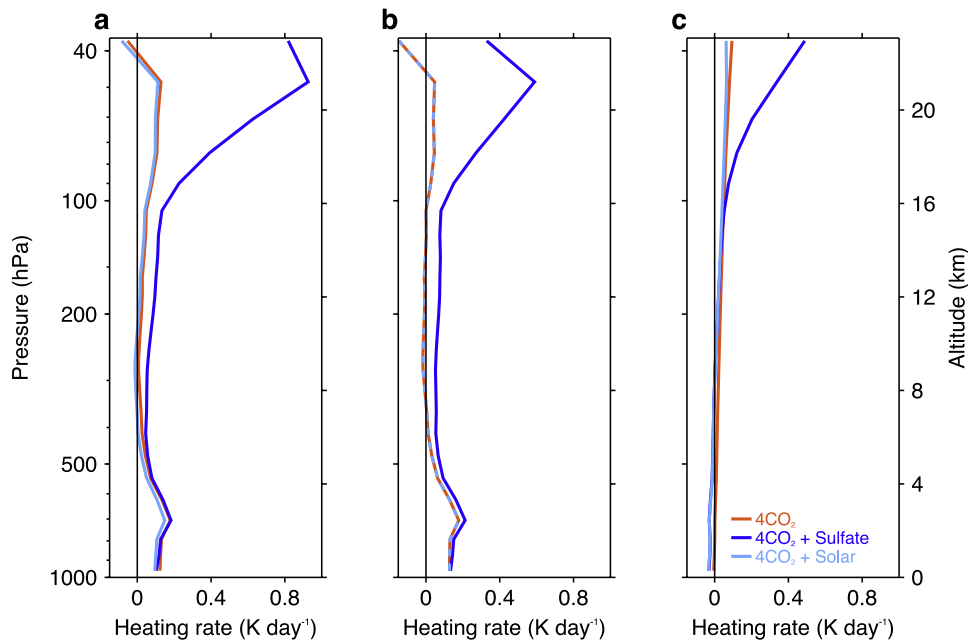
Figure 3. Vertical profiles of tropical-mean instantaneous radiative heating rate perturbations compared to the control simulation for (a) total (0.25–50 μm), (b) longwave (4–50 μm) and (c) visible and near-infrared (0.25–4 μm).

itself and due to increased LW emission from the warmer stratosphere.

Increased tropospheric warming with height has been shown to be important for changes to the tropical overturning circulation, and consequently for tropical precipitation. In greenhouse gas warming scenarios, mean tropical precipitation is expected to increase, but the tropical overturning circulation is expected to decrease [10, 11]. This change in circulation can be explained by changes in tropospheric stability which cause cooling in regions of ascent and warming in regions of descent [12, 13].

Changes in the tropical temperature profile therefore drive changes in the tropical circulation, as suggested for CO_2 increases [10–14]. Since stratospheric sulfate geoengineering also produces upper-tropospheric warming, a weakening of the tropical circulation would also be expected in the '4CO_2 + Sulfate' simulation. There may also be a contribution from upper-tropospheric radiative heating, which reduces upward latent heat flux by reducing the net radiative cooling of the atmosphere [6, 10]. Figure 4 shows pressure vertical velocity at 500 hPa (ω_{500}), a commonly used proxy for the strength of the tropical circulation [10, 11], binned into percentiles. There is little change in any percentile for the '4CO_2 + Solar' simulation, whereas both the '4CO_2' and '4CO_2 + Sulfate' simulations show a clear downwelling (positive) anomaly in upwelling regions (negative ω_{500}) and an upwelling (negative) anomaly in downwelling regions (positive ω_{500}). This is consistent with our hypothesis regarding the importance of tropospheric stability, in the absence of surface temperature change, for determining the strength of the tropical overturning circulation.

Such a weakening in the tropical circulation would be expected to reduce precipitation rates. Figure 4(c) shows that '4CO_2 + Sulfate' does indeed reduce tropical-mean

precipitation by 0.25 mm d^{-1}. This is approximately double the reduction in '4CO_2 + Solar'.

Increasing atmospheric CO_2 concentrations increases the radiative flux at the top-of-the-atmosphere more than at the surface, introducing a so-called 'fast' response whereby the troposphere rapidly adjusts to this net radiative heating by reducing the latent heat flux from the surface [24, 25]. By fitting a linear trend to the annual evolution of precipitation and temperature anomalies in '4CO_2', we see that the fast precipitation response to CO_2 (when the tropical-mean temperature anomaly is zero) is −0.14 mm d^{-1} (figure 4(c)). This is very similar to the '4CO_2 + Solar' response. In '4CO_2 + Solar' precipitation is reduced because using solar irradiance reductions to counterbalance the top-of-the-atmosphere radiative forcing from CO_2 results in a radiative heating of the atmosphere and reduces evaporation (and hence precipitation). In the long-term, increasing CO_2 enhances tropical precipitation due to enhanced tropospheric radiative cooling [10].

However, '4CO_2 + Sulfate' includes an additional effect on precipitation to the fast radiative response of CO_2. The tropical circulation is weakened in such a way that convective activity in upwelling regions is suppressed and tropical-mean precipitation is reduced. This is consistent with studies of the effect of net atmospheric heating on precipitation rates [29]. It has been shown that the 'greenhouse effect' of geoengineering aerosols on the net LW tropospheric heating is important in determining the precipitation response, and that the precipitation response is therefore larger than when geoengineering is simulated as solar dimming [30]. Here we show the importance of the heating of the upper tropical troposphere for the tropospheric static stability and the strength of the tropical overturning.
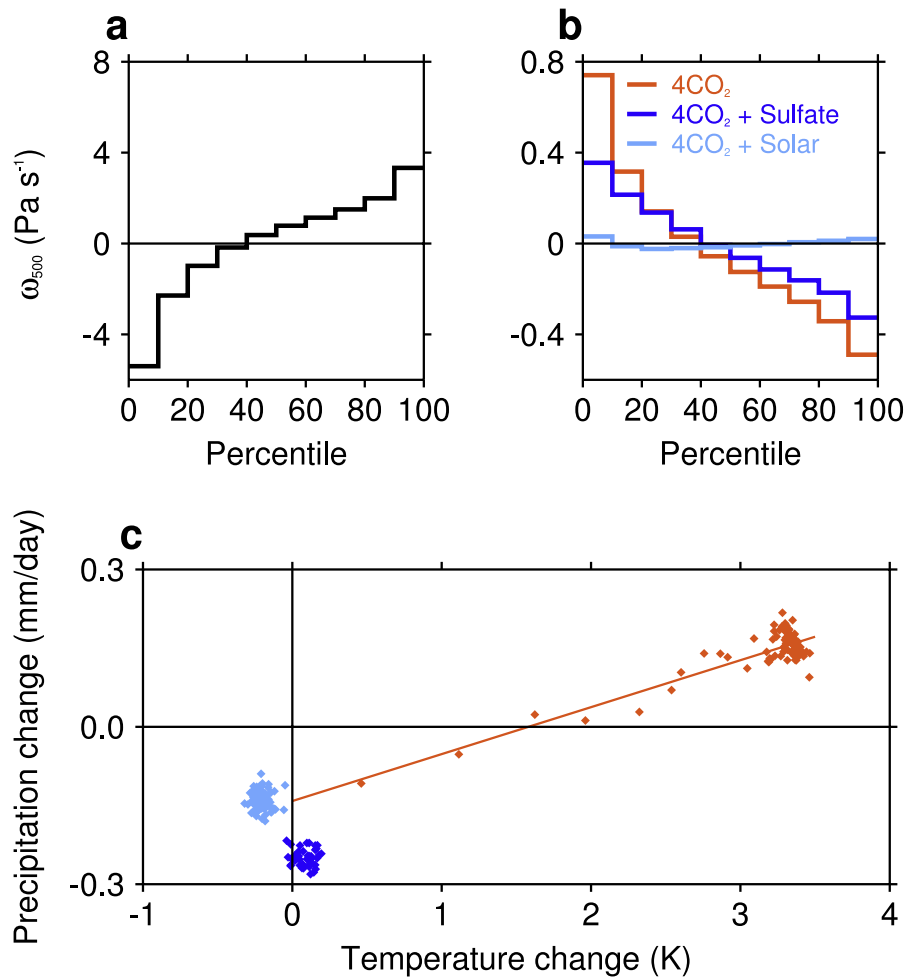
Figure 4. Percentiles of tropical-mean pressure vertical velocity at 500 hPa (ω_{500}) for (a) control and (b) response compared to the control simulation in $4CO_2$ and geoengineering simulations. (c) Scatter plot of annual-mean tropical-mean surface temperature and precipitation anomalies relative to the control simulation, showing the fast radiative response to CO_2 where the linear fit intercepts the temperature axis.

This study uses a relatively small aerosol median radius, which is likely unrealistic because large injections of aerosol into the stratosphere enhance coagulation processes. Larger aerosols have a lower scattering efficiency and produce stronger stratospheric heating [31]. Therefore it is likely that the magnitude of the upper-tropospheric heating and precipitation reductions in the $4CO_2$ + Sulfate simulation are underestimated. Since this study uses a single global climate model of intermediate complexity, quantitative assessment of this effect on the tropical upwelling is difficult. Further investigation, within the multi-model GeoMIP framework [15], for example, will help ascertain the robustness of, and model uncertainty in, this mechanism.

4. Conclusions

This letter has compared the impacts on the tropical temperature profile and overturning circulation of geoengineering with sulfate aerosol ('$4CO_2$ + Sulfate') and solar dimming ('$4CO_2$ + Solar'). Removing surface warming removes surface-mediated effects on precipitation, unmasking the fast radiative response of precipitation to CO_2 increases

in the '$4CO_2$ + Solar' case (figure 4(c)), as suggested by Bony *et al* [14]. Sulfate geoengineering, however, enhances the fast response of precipitation to CO_2 increases. When stratospheric aerosol geoengineering is represented more realistically using a sulfate aerosol layer there is additional atmospheric heating from the aerosol layer which weakens the tropical circulation, suppressing convection and further reducing precipitation. Consequently, though stratospheric aerosol geoengineering could be used compensate for the surface warming produced by CO_2 globally, or even regionally, there is a tropical precipitation change of the opposite sign to and greater in magnitude than the long-term response to CO_2. Climate model simulations representing geoengineering as solar dimming [16–18] do not represent this effect.

Such climatological precipitation changes are of considerable importance in regions vulnerable to droughts and floods, as well as being drivers of changes in agricultural production. Precipitation changes can be caused by changes in the atmospheric circulation as well as by direct radiative effect such as changes in evaporation rates. The results presented here highlight the importance of assessing the

impacts of stratospheric aerosol geoengineering on large-scale circulation regimes, as well as on global-mean parameters, to appropriately characterize the effectiveness of such a climate intervention.

Acknowledgments

References

[1] Meehl G *et al* 2007 *Global climate projections Climate Change 2007: The Physical Science Basis. Contribution of Working Group I to the 4th Assessment Report of the Intergovernmental Panel on Climate Change* (Cambridge: Cambridge University Press) pp 747–845

[2] Crutzen P J 2006 Albedo enhancement by stratospheric sulfur injections: a contribution to resolve a policy dilemma? *Clim. Change* **77** 211–20

[3] The Royal Society 2009 *Geoengineering the Climate: Science Governance and Uncertainty* (London: The Royal Society)

[4] Rasch P J, Tilmes S, Turco R P, Robock A, Oman L, Chen C-C, Stenchikov G L and Garcia R L 2008 An overview of geoengineering of climate using stratospheric sulphate aerosols *Phil. Trans. R. Soc.* A **366** 4007–37

[5] Jones A, Haywood J M, Boucher O, Kravitz B S and Robock A 2010 Geoengineering by stratospheric SO_2 injection: results from the Met Office HadGEM2 climate model and comparison with the Goddard Institute for Space Studies ModelE *Atmos. Chem. Phys.* **10** 5999–6006

[6] Allen M R and Ingram W J 2002 Constraints on future changes in climate and the hydrologic cycle *Nature* **419** 224–32

[7] Bala G, Duffy P B and Taylor K E 2008 Impact of geoengineering schemes on the global hydrological cycle *Proc. Natl Acad. Sci.* **105** 7664–9

[8] Robock A, Oman L and Stenchikov G L 2008 Regional climate responses to geoengineering with tropical and Arctic SO_2 injections *J. Geophys. Res.* **113** D16101

[9] Ricke K L, Morgan M G and Allen M R 2010 Regional climate response to solar-radiation management *Nature Geosci.* **3** 537–54

[10] Held I M and Soden B J 2006 Robust responses of the hydrological cycle to global warming *J. Clim.* **19** 5686–99

[11] Vecchi G A and Soden B J 2007 Global warming and the weakening of the tropical circulation *J. Clim.* **20** 4316–40

[12] Knutson T R and Manabe S 1995 Time-mean response over the tropical pacific to increased CO_2 in a coupled ocean–atmosphere model *J. Clim.* **8** 2181–99

[13] Ma J, Xie S-P and Kosaka Y 2012 Mechanisms for tropical tropospheric circulation change in response to global warming *J. Clim.* **25** 2979–94

[14] Bony S, Bellon G, Klocke D, Sherwood S, Fermepin S and Denvil S 2013 Robust direct effect of carbon dioxide on tropical circulation and regional precipitation *Nature Geosci.* **6** 447–51

[15] Kravitz B, Robock A, Boucher O, Schmidt H, Taylor K E, Stenchikov G and Schulz M 2011 The Geoengineering Model Intercomparison Project (GeoMIP) *Atmos. Sci. Lett.* **12** 162–7

[16] Schmidt H, Alterskjær K, Karam D B, Boucher O, Jones A and Kristjansson J E 2012 Solar irradiance reduction to counteract radiative forcing from a quadrupling of CO_2: climate responses simulated by four earth system models *Earth Syst. Dyn.* **3** 63–78

[17] Kravitz B *et al* 2013 Climate model response from the Geoengineering Model Intercomparison Project (GeoMIP) *J. Geophys. Res.* **118** 8320–32

[18] Tilmes S *et al* 2013 The hydrological impact of geoengineering in the Geoengineering Model Intercomparison Project (GeoMIP) *J. Geophys. Res.* **118** 11036–58

[19] Forster P M, Blackburn M, Glover R and Shine K P 2000 An examination of climate sensitivity for idealised climate change experiments in an intermediate general circulation model *Clim. Dyn.* **16** 833–49

[20] Morcrette J-J 1991 Radiation and cloud radiative properties in the European centre for medium range weather forecasts forecasting system *J. Geophys. Res.* **96** 9121–32

[21] Rothman L S *et al* 1987 The HITRAN database: 1986 edition *Appl. Opt.* **26** 4058–97

[22] Uppala S M *et al* 2005 The ERA-40 re-analysis *Q. J. R. Meteorol. Soc.* **131** 2961–3012

[23] Niemeier U, Schmidt H and Timmreck C 2011 The dependency of geoengineered sulfate aerosol on the emission strategy *Atmos. Sci. Lett.* **12** 189–94

[24] Gregory J and Webb M 2008 Tropospheric adjustment induces a cloud component in CO_2 forcing *J. Clim.* **21** 58–71

[25] Bala G, Caldeira K and Nemani R 2009 Fast versus slow response in climate change: implications for the global hydrological cycle *Clim. Dyn.* **35** 423–34

[26] Ramachandran S, Ramaswamy V, Stenchikov G L and Robock A 2000 Radiative impact of the Mount Pinatubo volcanic eruption: lower stratospheric response *J. Geophys. Res.* **105** 24409–29

[27] Ramaswamy V and Freidenreich S M 1991 Solar radiative line-by-line determination of water vapor absorption and water cloud extinction in inhomogeneous atmospheres *J. Geophys. Res.* **96** 9133–57

[28] English J M, Toon O B and Mills M J 2012 Microphysical simulations of sulfur burdens from stratospheric sulfur geoengineering *Atmos. Chem. Phys.* **12** 4775–93

[29] Liepert B G and Previdi M 2009 Do models and observations disagree on the rainfall response to global warming? *J. Clim.* **22** 3156–66

[30] Niemeier U, Schmidt H, Alterskjaer K and Kristjánsson J E 2013 Solar irradiance reduction via climate engineering: impact of different techniques on the energy balance and the hydrological cycle *J. Geophys. Res.* doi:10.1002/2013JD020445

[31] Ferraro A J, Highwood E J and Charlton-Perez A J 2011 Stratospheric heating by potential geoengineering aerosols *Geophys. Res. Lett.* **38** L24706